Progress In Electromagnetics Research C, Vol. 51, 55–62, 2014

A Fast Hybrid WCIP and FDTLM Approach to Study Inhomogeneous Circuits

Asmaa Zugari[1, *], Nathalie Raveu[2], Caroline Girard[2], Henri Baudrand[2], and Mohsine Khalladi[1]

Abstract—The hybrid approach based on the coupling of the Wave Concept Iterative Procedure method and the Frequency Domain Transmission Line Matrix method is improved. The proposed method reduces the computation time by solving waves at the planar circuit interface: the volumic method is replaced by an equivalent surface condition. Thanks to this new approach, planar circuits presenting inhomogeneous dielectric substrates are studied. The proposed approach is compared to other methods on several examples.

1. INTRODUCTION

Microwave circuits can be accurately analyzed using methods based on Maxwell's equations. Nowadays, many numerical techniques are available. Using hybrid methods is a powerful way to solve efficiently electromagnetic problems.

The Wave Concept Iterative Procedure (WCIP) is a method of moments [1], based on waves concept first introduced by Baudrand in 1995 [2, 3]. It consists of electromagnetic fields combined to define incident and reflected waves around circuits interfaces. The solution is obtained via an iterative procedure instead of a direct solution. This method is restricted to the study of circuits with homogenous substrates, since modes must be defined around circuits interfaces.

The Frequency Domain Transmission Line Matrix (FDTLM) method [4] is a numerical technique suitable for electromagnetic field phenomena simulation in microwave structures. Its concept was first introduced by Jin and Vahldieck in 1992 [5, 6]. It is based on the analogy between voltages/currents behavior in an interconnected transmission line network and electric/magnetic fields in a defined medium. Its major advantage is the facility of the electromagnetic field simulation in inhomogeneous and complex media. This method computes electromagnetic fields on rectangular meshes, and therefore, is particularly well suited for the coupling with the WCIP. A symmetrical FDTLM node is derived from Maxwell's equations using centered differencing and averaging [7, 8]. Its main drawback remains the computation time [9].

Successful tests have been carried out previously, hybridizing the WCIP with the TDTLM [10] and FDTLM [11, 12]. In this paper, the coupling between these two methods is improved through two ways:

- The conversion of unknowns between voltages and waves of [11, 12] is no longer necessary, since the FDTLM node is here reformulated to correspond to the WCIP unknowns;
- The FDTLM volume operator is replaced by an equivalent surface condition that allows computation time saving compared to [11, 12].

Hybridization theory between the WCIP and the FDTLM is provided, and herafter validated through two examples in homogeneous and inhomogeneous cases.

Received 15 May 2014, Accepted 7 June 2014, Scheduled 16 June 2014

* Corresponding author: Asmaa Zugari (asmaa.zugari@gmail.com).

[1] Electronics and Microwaves Research Group (EMG), Laboratory Systems of Information and Telecommunications (LaSIT), Faculty of Sciences, Abdelmalek Essaadi University, Tetuan, Morocco. [2] INPT, UPS, LAPLACE, ENSEEIHT, University of Toulouse, Toulouse, France.

2. WCIP/FDTLM FORMULATION

2.1. WCIP Review

The WCIP [1] is based on recurrence relations between the reflected **A** and the incident **B** waves seen from circuits interfaces:

$$\begin{cases} \mathbf{A} = \dfrac{1}{2\sqrt{Z_0}}(\mathbf{E_T} + Z_0\mathbf{J_T}), \\ \mathbf{B} = \dfrac{1}{2\sqrt{Z_0}}(\mathbf{E_T} - Z_0\mathbf{J_T}), \end{cases} \tag{1}$$

where Z_0 is an arbitrarily chosen impedance. $\mathbf{E_T}$ and $\mathbf{H_T}$ are the tangential electric and magnetic fields. ($\mathbf{J_T} = \mathbf{H_T} \wedge \mathbf{n}$), $\mathbf{J_T}$ is the tangential current density. $\mathbf{n}$ is the outward unit vector normal to the considered interface.

The analytical expression of the iterative process involves a system of two equations: one written in the spatial domain (2), characterizing the boundary conditions at the interface of the structure through the operator $\hat{S}$; the other expressed in the modal domain (3), describing the upper and lower media through the operator $\hat{\Gamma}$ [13]. A Fast Modal Transform (FMT), and its inverse (FMT^{-1}), ensure conversions between both domains [14]. To use these conversions, the mesh must be rectangular and regular, the circuit dimensions must meet these specifications to be solved with this hybrid method. The iterative process is defined by:

$$\mathbf{A} = \hat{S}\mathbf{B} + \mathbf{A}_0, \tag{2}$$

$$\tilde{\mathbf{B}} = \hat{\Gamma}\tilde{\mathbf{A}}, \tag{3}$$

where $\mathbf{A}_0$ is the localized excitation source, $\mathbf{A}$ and $\mathbf{B}$ are defined in the spatial domain, while $\tilde{\mathbf{A}}$ and $\tilde{\mathbf{B}}$ are defined in the modal domain.

The simulation result is gradually approached by successive iterations until convergence is reached.

2.2. Modified FDTLM

Changes in FDTLM are needed to facilitate the hybridization with the WCIP. The conventional FDTLM node has been adapted for wave interaction and is represented in Fig. 1.

The relation between the incident and reflected waves in the node is controlled by the FDTLM scattering matrix according to $\mathbf{B} = S^{\mathrm{FDTLM}}\mathbf{A}$. This matrix is derived from Maxwell's equations using centered differencing and averaging. Complete details of these developments can be found in [8, 15].

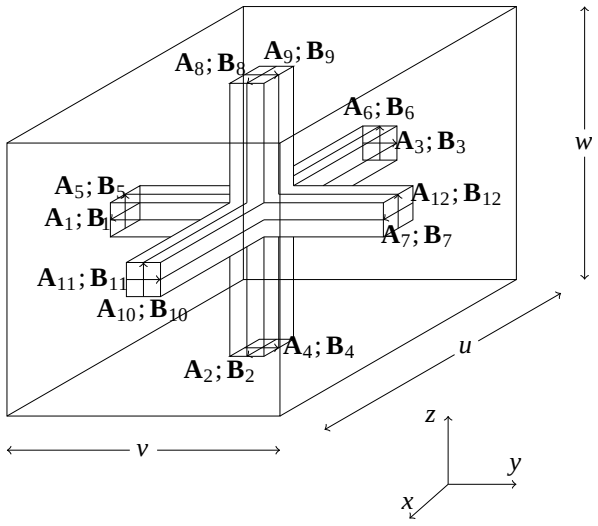

Figure 1. FDTLM node adapted to the WCIP waves definitions.

Thus, the scattering matrix of the FDTLM cell is defined in (4). This 12×12 node takes into account local variations in mesh size and lossy anisotropic media, with a conductivity, complex permittivity and complex permeability tensors, where:

$$a = b - d \qquad b = \frac{2}{(4 + Z_0 G_{e\alpha})}$$
$$c = b + d - 1 \quad d = \frac{2Z_0}{(4Z_0 + G_{m\beta})}$$

where

$$G_{ex} = (\sigma_{ex} + j\omega\varepsilon_x) \cdot \frac{v \cdot w}{u} \quad G_{mx} = (\sigma_{mx} + j\omega\mu_x) \cdot \frac{v \cdot w}{u}$$
$$G_{ey} = (\sigma_{ey} + j\omega\varepsilon_y) \cdot \frac{u \cdot w}{v} \quad G_{my} = (\sigma_{my} + j\omega\mu_y) \cdot \frac{u \cdot w}{v}$$
$$G_{ez} = (\sigma_{ez} + j\omega\varepsilon_z) \cdot \frac{u \cdot v}{w} \quad G_{mz} = (\sigma_{mz} + j\omega\mu_z) \cdot \frac{u \cdot v}{w}$$

with ω the angular frequency; ε_i the permittivity of the medium along i axis; μ_i the permeability of the medium along i axis; σ_{e_i} the electrical conductivity of the medium along i axis and σ_{m_i} the magnetic conductivity of the medium along i axis.

$$S^{\mathrm{FDTLM}} = \begin{array}{c} \begin{matrix} \alpha \\ \beta \end{matrix} \\ \begin{pmatrix} \mathbf{x} & \mathbf{x} & \mathbf{y} & \mathbf{y} & \mathbf{z} & \mathbf{z} & \mathbf{z} & \mathbf{y} & \mathbf{x} & \mathbf{z} & \mathbf{y} & \mathbf{x} \\ \mathbf{z} & \mathbf{y} & \mathbf{z} & \mathbf{x} & \mathbf{x} & \mathbf{y} & \mathbf{x} & \mathbf{x} & \mathbf{y} & \mathbf{y} & \mathbf{z} & \mathbf{z} \\ & & & & & & & & & & & \\ a & b & d & 0 & 0 & 0 & 0 & 0 & b & 0 & -d & c \\ b & a & 0 & 0 & 0 & d & 0 & 0 & c & -d & 0 & b \\ d & 0 & a & b & 0 & 0 & 0 & b & 0 & 0 & c & -d \\ 0 & 0 & b & a & d & 0 & -d & c & 0 & 0 & b & 0 \\ 0 & 0 & 0 & d & a & b & c & -d & 0 & b & 0 & 0 \\ 0 & d & 0 & 0 & b & a & b & 0 & -d & c & 0 & 0 \\ 0 & 0 & 0 & -d & c & b & a & d & 0 & b & 0 & 0 \\ 0 & 0 & b & c & -d & 0 & d & a & 0 & 0 & b & 0 \\ b & c & 0 & 0 & 0 & -d & 0 & 0 & a & d & 0 & b \\ 0 & -d & 0 & 0 & b & c & b & 0 & d & a & 0 & 0 \\ -d & 0 & c & b & 0 & 0 & 0 & b & 0 & 0 & a & d \\ c & b & -d & 0 & 0 & 0 & 0 & 0 & b & 0 & d & a \end{pmatrix} \end{array} \tag{4}$$

The conditions of connection between the nodes are similar to those of the classical operator $\hat{S}$ of the WCIP [13], they are given by the following relationship:

$$\mathbf{A} = C\mathbf{B} \tag{5}$$

where the transmission between adjacent nodes is ensured through insulated node faces, and total reflection is ensured over metallic node faces.

2.3. Hybridization between the WCIP and the FDTLM

The (FDTLM/WCIP) hybridization aims at qualifying simple or multilayered circuits with or without inhomogeneities. First encouraging results were obtained in 2d in [16]. Let us consider the circuit illustrated in Fig. 2.

The WCIP method is used to characterize medium 1 (up to the interface Ω), where homogeneous medium is considered (vacuum) on a surface mesh. The FDTLM is used below it, in medium 2 (down to the interface Ω), which might be inhomogeneous. The boundary conditions on Ω are taken into account by the iterative method in a conventional manner. The mesh used on the interface Ω for the WCIP and the FDTLM is the same. Initially, the structure is excited by a single spatial localized source, generating waves on both sides of the interface. In the upper medium (subscript 1), the iterative method is conventionally applied. In the lower medium (subscript 2), waves are calculated with the FDTLM.

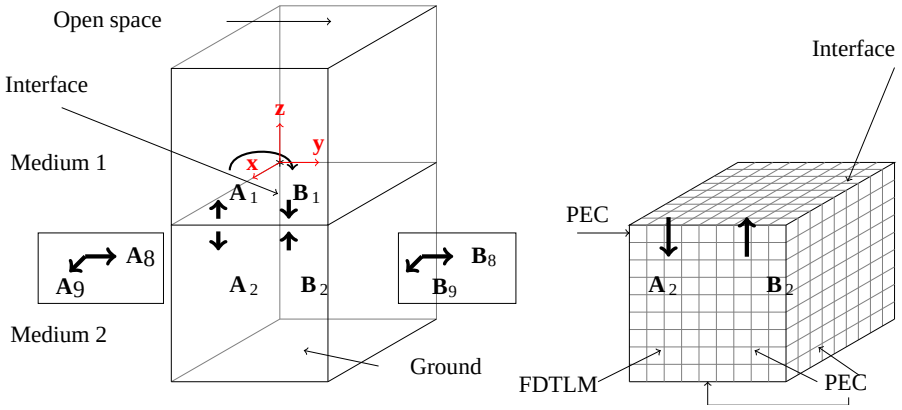

Figure 2. FDTLM/WCIP hybridization representation when a circuit is printed on the interface Ω.

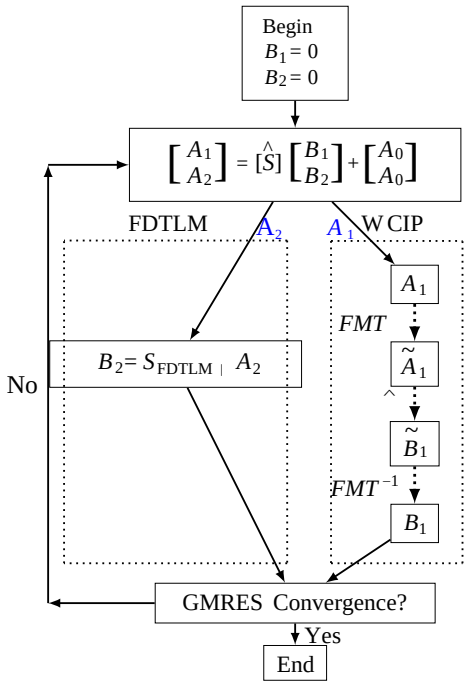

Figure 3. Diagram of the hybrid process.

The hybridization is ensured with the correspondence of $(\mathbf{A_{2x}}, \mathbf{A_{2y}}, \mathbf{B_{2x}}, \mathbf{B_{2y}})$ and $(\mathbf{A_9}, \mathbf{A_8}, \mathbf{B_9}, \mathbf{B_8})$. To improve computation time, solution in the FDTLM volumic mesh is reduced to a frontier relation that is detailed next.

B and **A** waves are now separated into the frontier unknowns, denoted F (at the interface Ω), and the inner volume unkowns, denoted i ($i = [1-7] \cup [10-12]$). The scattering matrix (4) can be detailed with these notations:

$$\begin{pmatrix} \mathbf{B_F} \\ \mathbf{B_i} \end{pmatrix} = \begin{pmatrix} S_{FF} & S_{Fi} \\ S_{iF} & S_{ii} \end{pmatrix} \begin{pmatrix} \mathbf{A_F} \\ \mathbf{A_i} \end{pmatrix} \tag{6}$$

with $\mathbf{A_F} = (\mathbf{A_9} \quad \mathbf{A_8})_\Omega$ and $\mathbf{B_F} = (\mathbf{B_9} \quad \mathbf{B_8})_\Omega$ denoting the reflected and the incident waves on the interface Ω and $\mathbf{A_i}$, $\mathbf{B_i}$ elsewhere ($i = [1-7] \cup [10-12]$).

Connection matrix (5) is satisfied for inner unknowns:

$$\mathbf{B_i} = C^{-1}\mathbf{A_i}. \tag{7}$$

The coupling of (6) and (7) leads to a surface operator $S_{\mathrm{FDTLM}|_\Omega}$:

$$\mathbf{B_F} = \underbrace{(S_{FF} + S_{Fi}(C^{-1} - S_{ii})^{-1} S_{iF})}_{S_{\mathrm{FDTLM}|_\Omega}} \mathbf{A_F}. \tag{8}$$

The process is depicted in Fig. 3. The solution of iterative system is performed by Generalized Minimal RESidual algorithm (GMRES) [17–19]. The computation time is improved with this surface FDTLM operator compared to [11].

3. NUMERICAL RESULTS

The proposed study concerns the calculation of the scattering parameters of a suspended T junction structure. An accurate description of the T junction is given, since the resonance frequency is very sensitive to the stub length and width. Consequently, results obtained for this example proves the accuracy of the technique. The proposed hybrid method will be compared with two numerical methods: the Finite Element Method (FEM) (obtained with the commercial software HFSS version 13.0.2) and the Method of Moments (MoM) (obtained with the commercial software MoMentum). Results are obtained on Intel Xeon machine 3.2 GHz, RAM 16 Go, 12 cores.

3.1. Homogeneous Case

The proposed WCIP/FDTLM approach is validated on a suspended T junction, enclosed in an opened metallic box (lateral faces are metalized but the top is opened and simulated with Radiation Boundary in HFSS). Dimensions are described in Fig. 4.

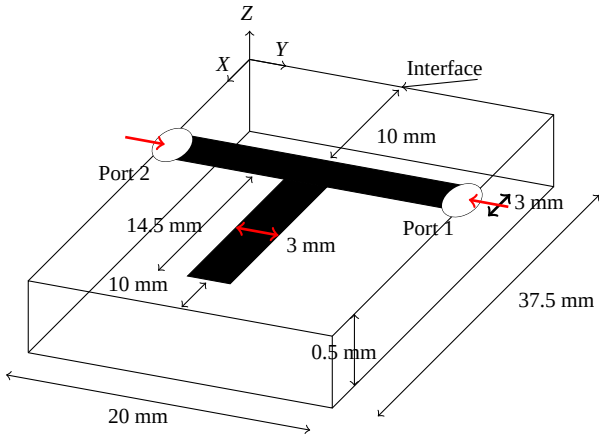

Figure 4. Suspended T junction circuit.

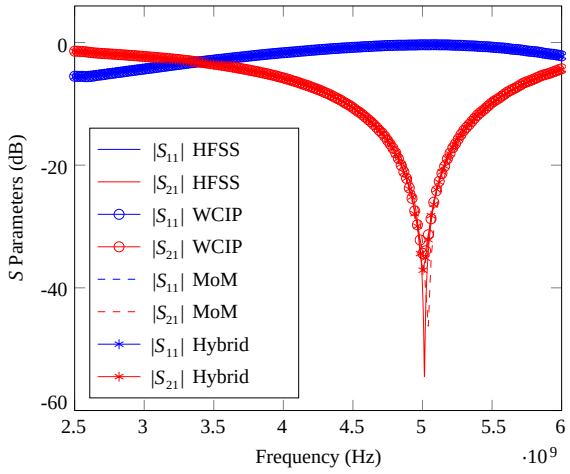

Figure 5. S parameters of the suspended T junction circuit for different numerical techniques.

Table 1. Computation time for the example of the suspended T junction circuit obtained with different numerical techniques.

Numerical methods	Computation Time	Number of unknowns
HFSS	29 s/Frequency	16974
WCIP	27 s/Frequency	768000
MoMentum	5.5 s/Frequency	178
Hybrid method	5.4 s/Frequency	116880

The structure was simulated with the hybrid approach to validate the proposed concept using a regular mesh of 0.25 mm length, while a regular mesh of 0.125 mm length is needed for the WCIP to reach the same accuracy at the resonant frequency.

The coefficients S_{11} and S_{12} are shown in Fig. 5, according to the frequency, for four numerical methods. Results are in good agreement. It is worth mentioning that the hybrid method results coincide with those of the WCIP and the MoM.

The results of the computation time per frequency for each method are shown in Table 1. Computation time is achieved at each frequency point independently, with a setup at each frequency, the maximum number of HFSS passes is 20, $\Delta S = 0.01$, the memory storage is 147 M. Generally, the convergence is reached around 7 or 8 passes. It can be observed that, the computation time of the hybrid method is similar to the WCIP alone and much lower than the HFSS one, but slightly higher than the MoMentum one. Furthermore, the hybrid method can deal with inhomogeneous media, which cannot be done with the WCIP or MoMentum.

3.2. Inhomogeneous Case

In a second example, a localized substrate of relative permittivity ε_r is inserted at the end of the stub (see Fig. 6), which shifts its resonant frequency. Its length and width are 6 mm with a height of 0.5 mm, the frequency step is of 0.001 GHz.

The calculated S parameters of the inhomogeneous structure with WCIP/FDTLM approach show a good agreement with the HFSS results as presented in Fig. 7 and Fig. 8, considering the resonant frequency of two different relative permittivities $\varepsilon_r = 2.2$ and $\varepsilon_r = 4.4$. This structure cannot be simulated with the WCIP alone (or MoMentum) as the substrate is inhomogeneous. This comparison justifies the efficiency of the algorithm.

It is remarkable from Table 2 that, the computation time of the hybrid method is, at least, 3.5 lower than the HFSS one with similar accuracy. Computation time is achieved at each frequency point independently, with a setup at each frequency, the maximum number of HFSS passes is 20, $\Delta S = 0.01$, the memory storage is 147 M. Generally, the convergence is reached around 7 or 8 passes. The hybrid method performances might also be improved through preconditioning [20].

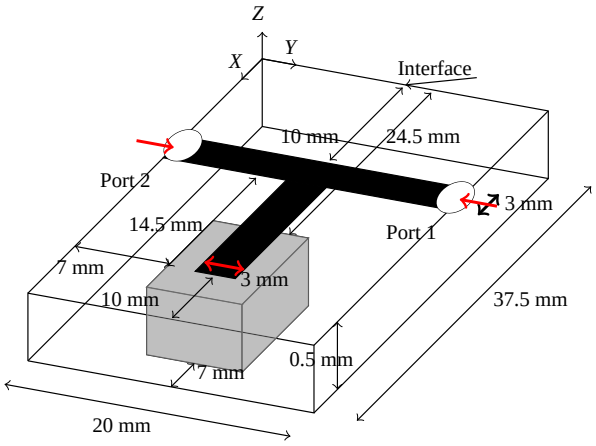

Figure 6. Inhomogeneous loaded T junction circuit.

Table 2. Computation time for the example of the inhomogeneous loaded T junction circuit ($\varepsilon_r = 4.4$) with the different numerical techniques.

Numerical methods	**Computation Time for $\varepsilon_r = 4.4$**	**Number of unknowns**
HFSS	22s/Frequency	24122
Hybrid method	5.9s/Frequency	116880

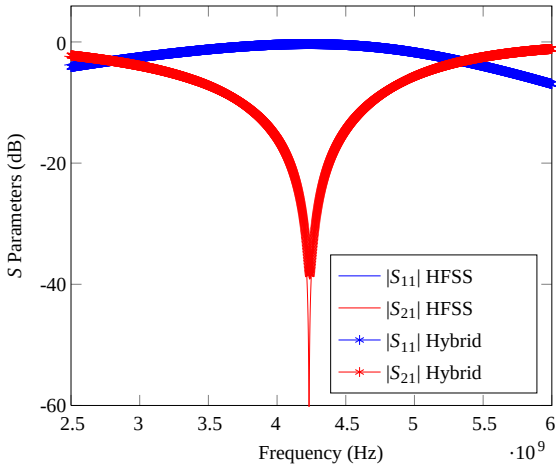

Figure 7. S parameters of the inhomogeneous loaded T junction circuit obtained with different numerical techniques ($\varepsilon_r = 2.2$).

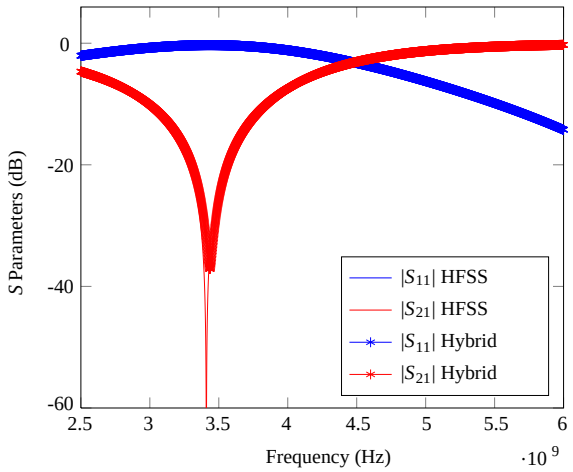

Figure 8. S parameters of the inhomogeneous loaded T junction circuit obtained with different numerical techniques ($\varepsilon_r = 4.4$).

4. CONCLUSION

The WCIP and the FDTLM hybridization is presented to extend the WCIP simulations to inhomogeneous layers in circuits study. The WCIP allows to study homogeneous structures with less computation memory than FDTLM requirement, thanks to waves description on a surface instead of a volume mesh in the FDTLM. FDTLM performs inhomogeneous simulation with similar surface mesh grid; both methods are therefore hybridized and tested on sensitive circuit examples. Results show the efficiency of the algorithm, with computation time, at least, 3.5 smaller than the commercial software HFSS.

ACKNOWLEDGMENT

The authors would like to thank Ronan Perrussel of the LAPLACE laboratory in INPT ENSEEIHT of the University of Toulouse, France, for his encouragement and helpful discussions.

REFERENCES

1. Zairi, H., A. Gharsallah, A. Gharbi, and H. Baudrand, "Analysis of planar circuits using a multigrid iterative method," *IEE Proc. — Microw. Antennas Propag.*, Vol. 135, No. 3, 231–236, Jun. 2006.
2. Azizi, M., H. Aubert, and H. Baudrand, "A new iterative method for scattering problems," *European Microwave Conf. Proc.*, Vol. 1, 255–258, Bologna, Italy, 1995.
3. N'gongo, R. S. and H. Baudrand, "A new approach for microstrip active antennas using modal FFT-algorithm," *IEEE Antennas and Propagation Society International Symposium*, Vol. 3, 1700–1703, Orlando, USA, 1999.
4. Hoefer, W. J. R., "The transmission-line matrix method — Theory and applications," *IEEE Transactions on Microwave Theory and Techniques*, Vol. 33, No. 10, 882–893, Oct. 1985.
5. Jin, H. and R. Vahldieck, "A frequency domain TLM method," *IEEE MTT-S International Microwave Symposium Digest*, 775–778, Albuquerque, USA, 1992.
6. Jin, H. and R. Vahldieck, "The frequency-domain transmission line matrix method — A new concept," *IEEE Transactions on Microwave Theory and Techniques*, Vol. 40, No. 12, 2207–2218, Dec. 1992.

7. Jin, H. and R. Vahldieck, "Direct derivations of TLM symmetrical condensed node and hybrid symmetrical condensed node from Maxwell's equations using centered differencing and averaging," *IEEE Transactions on Microwave Theory and Techniques*, Vol. 42, No. 12, 2554–2561, Dec. 1994.
8. Jin, H. and R. Vahldieck, "A new frequency-domain TLM symmetrical condensed node derived directly from Maxwell's equations," *IEEE MTT-S International Microwave Symposium Digest*, Vol. 2, 487–490, Orlando, USA, 1995.
9. Johns, D. and C. Christopoulos, "New frequency-domain TLM method for the numerical solution of steady-state electromagnetic problems," *IEE Proc. Sci. Meas. Technol.*, Vol. 141, No. 4, 310–316, 1994.
10. Fichtner, N., S. Wane, D. Bajon, and P. Russer, "Interfacing the TLM and the TWF method using a diakoptics approach," *IEEE MTT-S International Microwave Symposium Digest*, 57–60, Atlanta, USA, Jun. 2008.
11. Glaoui, M., H. Trabelsi, H. Zairi, A. Gharsallah, and H. Baudrand, "A new computationally efficient hybrid FDTLM-WCIP method," *International Journal of Electronics*, Vol. 96, No. 5, 537–548, 2009.
12. Glaoui, M., H. Zairi, and H. Trabelsi, "Contribution to the study of the planar circuits by a hybrid method (iterative method + FDTLM Method)," *5th International Conference: Sciences of Electronic, Technologies of Information and Telecommunications*, Tunisia, Mar. 22–26, 2009.
13. Titaouine, M., A. Gomes Neto, H. Baudrand, and F. Djahli, "WCIP method applied to active frequency selective surfaces," *Journal of Microwave and Optoelectronics*, Vol. 6, No. 1, 1–16, Jun. 2007.
14. Wane, S., D. Bajon, H. Baudrand, and P. Gamand, "A new full-wave hybrid differential-integral approach for the investigation of multilayer structures including nonuniformly doped diffusions," *IEEE Transactions on Microwave Theory and Techniques*, Vol. 53, No. 1, 200–214, Jan. 2005.
15. Zugari, A., M. Khalladi, M. I. Yaich, N. Raveu, and H. Baudrand, "A new approach: WCIP and FDTLM hybridization," *Mediterranean Microwave Symposium (MMS)*, Tanger, Marocco, Nov. 15–17, 2009.
16. Girard, C., A. Zugari, and N. Raveu, "2D FDTLM hybridization with modal method," *Progress In Electromagnetics Research B*, Vol. 55, 23–44, 2013.
17. Saad, Y. and M. Schultz, "A generalized minimal residual algorithm for solving non symmetric linear systems," *SIAM J. Sci. Stat. Comput.*, Vol. 7, 856–869, 1986.
18. Raveu, N. and H. Baudrand, "Improvement of the WCIP convergence," *IEEE APS, International Symposium on Antennas and Propagation and USNC/URSI National Radio Science*, 1–4, Charleston, USA Jun. 2009.
19. Raveu, N., L. Giraud, and H. Baudrand, "WCIP acceleration," *Asia-Pacific Microwave Conference Proceedings (APMC)*, 971–974, Dec. 7–10, 2010.
20. Raveu, N., J. Vincent, J. -R. Poirier, R. Perrussel, and L. Giraud, "Physically-based preconditioner for the WCIP," *Asia-Pacific Microwave Conference Proceedings (APMC)*, 1310–1312, Kaohsiung, Taiwan, Dec. 4–7, 2012.